Microchim Acta (2015) 182:1911–1916
DOI 10.1007/s00604-015-1525-5

ORIGINAL PAPER

Bovine serum albumin-stabilized gold nanoclusters as a fluorescent probe for determination of ferrous ion in cerebrospinal fluids via the Fenton reaction

Si Yang[1] · Zhongyao Jiang[1] · Zhenzhen Chen[1] · Lili Tong[1] · Jun Lu[1] · Jiahui Wang[1]

Received: 16 February 2015 / Accepted: 11 May 2015 / Published online: 22 May 2015

Abstract Gold nanoclusters (AuNCs) stabilized with bovine serum albumin were utilized as a fluorescent probe for ferrous ion. The detection scheme is based on the quenching of the fluorescence of the modified AuNCs by hydroxyl radical (•OH) that is generated in the Fenton reaction between Fe(II) and H_2O_2. Fe(II) can be quantified in the 0.08 to 100 μM concentration range, and the limit of detection is as low as 24 nM. The method also displays good accuracy and high sensitivity when employed to the determination of Fe(II) in rat cerebrospinal fluids (CSFs). When applied to CSFs of a rat model of Alzheimer's disease, it revealed enhanced levels of Fe(II) compared to a control, thereby showing the important physiological role of iron(II) in this disease.

Keywords Gold nanoclusters · Particle stabilization · Bovine serum albumin · Quenching · Ferrous ion · Fenton reaction · Cerebrospinal fluids

Electronic supplementary material The online version of this article (doi:10.1007/s00604-015-1525-5) contains supplementary material, which is available to authorized users.

✉ Zhenzhen Chen
zzchen@sdnu.edu.cn

✉ Lili Tong
lilitong@sdnu.edu.cn

[1] College of Chemistry, Chemical Engineering and Materials Science, Collaborative Innovation Center of Functionalized Probes for Chemical Imaging in Universities of Shandong, Shandong Provincial Key Laboratory of Clean Production of Fine Chemicals, Shandong Normal University, Jinan 250014, People's Republic of China

Introduction

Iron is the most affluent metal ion in cellular systems and of outstanding significance owing to its essential roles in biological systems [1]. Almost all cells employ iron ions as a cofactor for fundamental biochemical activities, such as oxygen transport, energy metabolism and DNA synthesis, based upon its ability to switch between the two most common redox states: ferrous, Fe(II) and ferric, Fe(III) [2]. Disruptions in iron homeostasis from both iron deficiency and overload account for some of the most common human diseases, such as anemia, Parkinson's syndrome, Alzheimer's disease and cancer [3]. Determination of iron content in biological systems is thus helpful for the diagnosis of some relevant diseases. However, much effort have been focused on the more stable and prevalent oxidation state, Fe^{3+}, and various probes specific for it have been reported [4, 5]. On the other hand, powerful method for detection of chemically more reactive species, Fe^{2+}, is rather limited.

The emergence of new kinds of fluorescent nanomaterials such as gold nanoclusters (AuNCs) is now generating new opportunities for targeting applications [6]. AuNCs [7] typically consist of several tens to a hundred of gold atoms, with small size regime comparable to Fermi wavelength of the conduction electrons. Since the continuous density of states breaks into discrete energy levels, AuNCs exhibit molecule-like properties in absorption and fluorescence [8]. Particularly, protein-templated AuNCs have attracted special attention due to their facile synthesis, strong fluorescence emission, high photostability, non-toxicity and high biocompatibility [9]. They have been studied widely, and free bilirubin [10] in blood serum samples and pathogenic bacteria [11] were detected using human serum albumin encapsulated gold nanoclusters (HSA-AuNCs). Some other biologically important molecules such as cystatin C [12], biothiols [13], glucose

[14], cysteine [15], xanthine [16], acetylcholinesterase activity [17] etc. have been successfully determined with bovine serum albumin-stabilized gold nanoclusters (BSA-AuNCs). Cyanide [18] and mercury ion [19] have also been determined based on the quenching of BSA-AuNC fluorescence.

In an investigation aimed at the development of a convenient and cost-effective procedure for assay of Fe^{2+} in biological and related circumstances, we established a fluorometric method with biocompatible BSA-AuNCs for the determination of ferrous ion. It is proven that the fluorescence of BSA-AuNCs is quenched by hydroxyl radical (•OH) [20], which is produced in the Fenton reaction between Fe^{2+} and H_2O_2. Then Fe^{2+} can be determined by the amount of generated •OH through fluorescent quenching. The method is sensitive, simple and rapid, and has demonstrated its feasibility by detecting ferrous ion in cerebrospinal fluids (CSFs). Due to the importance of iron in inflammation and oxidative stress that occurs with aging and, particularly, in Alzheimer's disease (AD) [21], we selected rat model of AD and determined ferrous ion in CSFs. The results showed enhanced CSFs ferrous ion content compared with control, which proved marked disease-associated changes in the iron content of the AD brain.

Experimental

Chemicals and reagents

Bovine serum albumin (BSA) and ascorbate oxidase (AO) were purchased from Sigma-Aldrich (http://www.sigmaaldrich.com). Chloroauric acid ($HAuCl_4 \cdot 4H_2O$), ferrous chloride ($FeCl_2$), sodium acetate trihydrate ($CH_3COONa \cdot 3H_2O$), acetic acid (CH_3COOH), ascorbic acid (AA) and hydrogen peroxide (H_2O_2) were purchased from Sinopharm Chemical Reagent Co. Ltd. (http://www.sinoreagent.com). The stock solution of H_2O_2 was freshly diluted from 30 % solution. All other chemicals, such as ferric chloride ($FeCl_3$), were of analytical grade and used without further purification. All solutions were prepared with water purified by a Milli-Q Purification System (http://www.merckmillipore.com/CN/en).

Synthesis and characterization of BSA-AuNCs

BSA-stabilized gold nanoclusters were synthesized in aqueous solution according to a previous publication [22]. In a typical experiment, all glassware used in the experiments was cleaned in a bath of freshly prepared aqua regia (HCl : HNO_3=3 : 1, V : V), and rinsed thoroughly with purified water prior to use. 15.0 mL aqueous $HAuCl_4$ solution (10 mM) was added to BSA solution (15.0 mL, 50 mg · mL^{-1}) under vigorous stirring at 37 °C. Two minutes later, 1.5 mL of 1 M NaOH solution was introduced and the mixture was allowed to incubate at 37 °C under vigorous stirring for 24 h. The color of the solution changed from light yellow to light brown, and then to deep brown. The solution was then dialyzed using a Solarbio MD44 dialysis bag (Molecular Weight Cut-off: 8000–14,000, www.shsolarbio.com) in 1 L double distilled water for 48 h to remove unreacted $HAuCl_4$ or NaOH, and the double distilled water was changed totally every 12 h. The final solution was diluted to 200 mL with purified water and stored at 4 °C in refrigerator. The morphological characterization of BSA-AuNCs was performed by high-resolution transmission electron microscopy (HR-TEM), images were taken with a JEOL JEM2100F microscope operated at 200 kV (Japan electron optics laboratory Co., Ltd, www.jeol.co.jp/en/). As for the synthesis reproducibility of and characterization BSA-AuNCs, see Electronic Supplementary Material (ESM).

Analytical procedures

The fluorescence measurements were performed on a Perkin Elmer LS-55 spectrofluorometer (www.perkinelmer.com.cn) equipped with a quartz cell (1 cm × 1 cm) in the fluorescence mode. For fluorescence detection of Fe^{2+}, appropriate amount of H_2O_2 and different concentrations of ferrous ion were added to an aliquot of 3 mL NaAc-HAc buffer (pH 5.70) solutions containing BSA-AuNCs (400 μL), which were placed in 5 mL colorimetric tubes. The mixtures were incubated at room temperature for 5 min before the spectral measurements. Finally, the fluorescence intensity of the test solution (F) and the blank solution (F_0) were recorded, in which F and F_0 are the maximum emission intensities of the BSA-AuNCs system in the presence and absence of Fe^{2+}, respectively.

Sample treatment and determination

Preparation of rat cerebrospinal fluids (CSFs) samples: Two groups of Wistar female rats were used, that is, animal model group of AD and control group (ESM). Each rat was anaesthetized with 0.8 mL of 3.5 % chloral hydrate dissolved in normal saline [23], and the CSFs samples were collected using a microinjector, whose needle was connected with a plastic pipe terminated in another needle. The CSFs samples were centrifugated at 1000 rpm for 5 min, the resulting supernatants were collected for the following detection experiments.

As for the fluorescence detection of ferrous ion in biological samples, appropriate amount of H_2O_2 and different amount of sample solution were added to an aliquot of 3 mL NaAc-HAc buffer (pH 5.70) solutions containing BSA-AuNCs (400 μL), plus certain amount of ascorbate oxidase (AO), which were placed in 5 mL colorimetric tubes. Then fluorescence intensity was recorded using the LS-55 spectrofluorometer.

Data were expressed as the mean±standard deviation. All experiments were repeated three times, and the data were calculated with Microsoft Excel.

Results and discussion

The fluorescent probe design

Among noble-metal nanoclusters, BSA-AuNCs are more prominent for bioanalysis due to their small size, excellent stability and biocompatibility. The working principle of fluorometric assay of Fe^{2+} is schematically represented in Scheme 1. BSA-AuNCs exhibit strong fluorescence, arising from intraband transitions of free electrons of the BSA-AuNCs [24]. In the presence of •OH, which is produced by Fenton reaction between Fe^{2+} and H_2O_2, the fluorescence intensity of the BSA-AuNCs can decrease significantly, attributable to the oxidation of Au(0) to Au(I) by •OH [20]. Thus it is possible for us to fabricate a facile means with BSA-AuNCs for the detection of Fe^{2+} ion in the presence of H_2O_2.

Detection of Fe^{2+} using BSA-AuNCs as fluorescent probe

In order to establish the proof-of-concept for our bioassay strategy outlined in Scheme 1, we conducted an experiment and evaluated the fluorescence change resulted from the interaction between BSA-AuNCs and •OH. As can be seen from Fig. 1, the emission spectrum of BSA-AuNCs (TEM image showed the average size is about 2 nm, Electronic Supplementary Material, Fig. S1) displayed an emission peak at around 638 nm upon excitation at 490 nm. Addition of Fe^{2+}/H_2O_2 significantly quenched the fluorescence of BSA-AuNCs, while addition of Fe^{2+} or H_2O_2 hardly changes the fluorescence of BSA-AuNCs. The photographs of the four samples under UV light (inset, Fig. 1) also coincided with the fluorescence variation. The evolution of fluorescence intensity of the four solutions mentioned above demonstrated the feasibility of the strategy. The same effect was obtained as AuNCs decorated silica particles described in reference [20], but the synthesis of BSA-AuNCs is simpler, and no fluorescent dye is needed. Consequently, the fluorescent procedure can be established for the low-cost and simple detection of Fe^{2+}, using biocompatible BSA-AuNCs as fluorescent probe.

The response of the fluorescent probe is usually affected by the media pH, temperature, and the reaction time. Therefore, in order to achieve sensitive detection of Fe^{2+}, effects of these parameters were studied and optimized. pH is a crucial factor for the detection system, and we find that stability of BSA-AuNCs will change across pH range (Electronic Supplementary Material, Fig. S2) because of BSA denaturation, but the fluorescence of BSA-AuNCs remains the highest when pH ranges between 5.4 and 6.0. We then explored the effect of

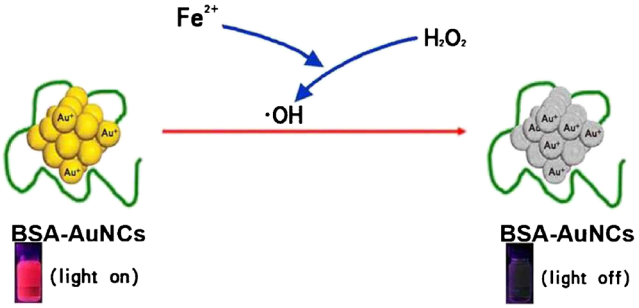

Scheme 1 Schematic illustration of fluorescent response of BSA-AuNCs to •OH (which is produced by Fenton reaction between Fe^{2+} and H_2O_2)

pH on the fluorescence difference ($\Delta F=F_0 - F_1$) of BSA-AuNCs in the absence (F_0) and presence (F_1) of Fe^{2+}. Correspondingly, as shown in Fig. 2a, the fluorescence intensity revealed the largest difference when pH of the media was in the range of 5.5–6.0. In weak acidic media when pH was below 5.5, ΔF increased with pH because of the decreased extent of BSA denaturation which was used for the stabilization of the gold nanoclusters; then such a difference reduced gradually when pH was above 6.0, because of both the hydrolysis of Fe^{2+} in neutral condition and BSA denaturation in basic media. Investigation of the effect of temperature on the fluorescence difference showed a temperature-dependent manner, as illustrated in Fig. 2b, ΔF decreased with increased temperature higher than 25 °C, owing to the decomposition of H_2O_2. On the other hand, the reaction was rather rapid and ΔF almost reaches the plateau only after 5 mins' incubation (data not shown). Therefore, to get a high sensitivity for detection of Fe^{2+}, a comparatively weak acidic media with the pH 5.7 (HAc-NaAc buffer, 0.1 M) and 5 min at room temperature were chosen for further experiments.

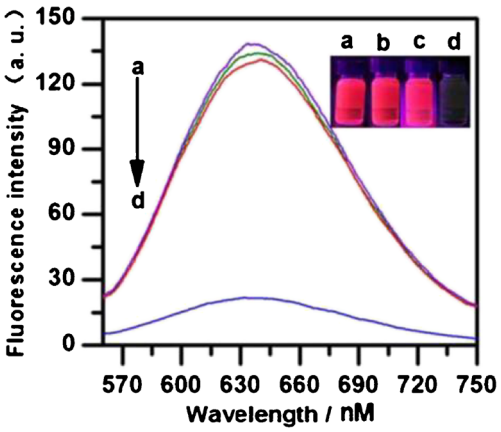

Fig. 1 The fluorescence spectra of BSA-AuNCs with different substrates (**a**) BSA-AuNCs only, (**b**) BSA-AuNCs with 100 μM Fe^{2+}, (**c**) BSA-AuNCs with 25 μM H_2O_2, (**d**) BSA-AuNCs with 100 μM Fe^{2+} and 25 μM H_2O_2

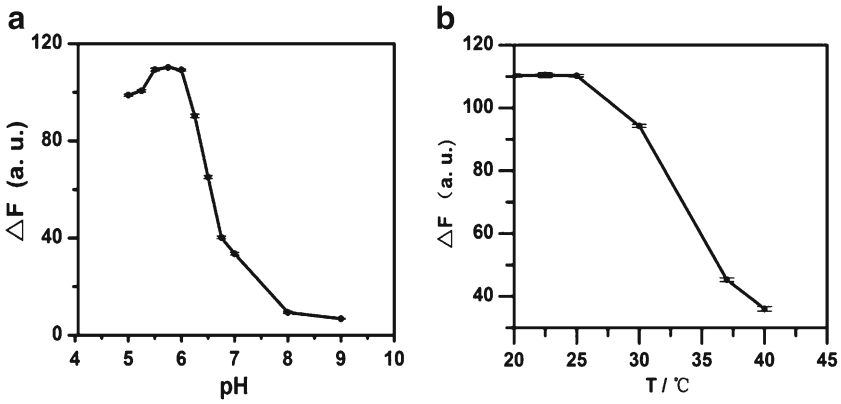

Fig. 2 Effect of pH (**a**) and temperature (**b**) on fluorescence change (ΔF) of BSA-AuNCs with 25 μM H_2O_2 in the absence (F_0) and presence (F_1) of Fe^{2+}, where $\Delta F=F_0-F_1$. The error bars represent the standard deviation of three measurements

Analytical parameters of the method

Under the optimum experimental conditions, the capability of the fluorometric approach for the evaluation of Fe^{2+} was investigated. Figure 3 displayed the fluorescence spectra of BSA-AuNCs with 25 μM H_2O_2 in the presence of different concentrations of Fe^{2+}. As illustrated, the fluorescence intensities decreased gradually with an increasing concentration of Fe^{2+}. Linear ranges of Fe^{2+} concentrations were obtained from 0.080 to 2.5 μM and from 5.0 to 100 μM with the limit of detection (LOD) down to 24 nM (Table 1). The corresponding regression equation of the working curve, correlation coefficient (R^2), relative standard deviation of 1.0 and 20 μM Fe^{2+} (RSD, separately determined in parallel six times), LOD (calculated by $3S_b/k$, which referred to the quotient between three times of the blank reagent's standard deviation where S_b=0.05, n=11, and k was the slope of the working curve) and the limit of quantification (LOQ, calculated by $10S_b/k$) of the fluorescent sensor were all listed in Table 1. We also tested the stability of the method, and found that BSA-AuNCs still retained its initial sensitivity toward Fe^{2+} after 60 days' storage at 4 °C in refrigerator. The good long-term stability attributes to the excellent stability of the AuNCs. Accordingly, with biocompatible fluorescent probe of BSA-AuNCs, the present fluorometric method can allow for the sensitive, repeatable and stable evaluation of Fe^{2+}.

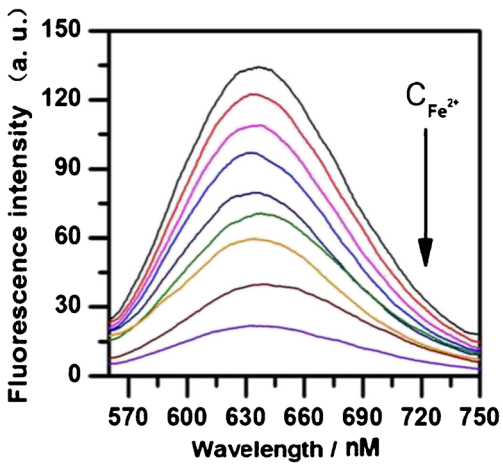

Fig. 3 Fluorescence responses of BSA-AuNCs to the coexistence of 25 μM H_2O_2 and different concentrations (μM) of Fe^{2+}: 0, 5, 15, 30, 50, 60, 70, 85, 100 (from top to bottom)

Selectivity of the fluorescent probe for Fe^{2+}

To evaluate the potential interference toward Fe^{2+} detection with BSA-AuNCs, the fluorescence response of Fe^{2+} (80 μM or none) together with BSA-AuNCs and 25 μM H_2O_2 was then investigated in the presence of competing ions or biomolecules. As shown in Fig. 4, 5000-fold excess of Na^+, 3000-fold excess of K^+, 500-fold excess of Ca^{2+}, Cr^{3+} and Mg^{2+}, 300-fold excess of Sn^{2+}, Pb^{2+}, 200-fold excess of glucose (Glu), 100-fold excess of glutathione (GSH), and 80-fold excess of cysteine (Cys), 50-fold excess of Fe^{3+}, 6-fold excess of Mn^{2+}, 4-fold excess of Cu^{2+}, the signal perturbation on Fe^{2+} detection was generally less than ± 5.0 % (Electronic Supplementary Material, Fig. S3 showed the fluorescence spectra of BSA-AuNCs together with 25 μM H_2O_2 and different species). Although Mn^{2+} and Cu^{2+} may interfere with the Fe^{2+} determination, their content are rather low under biological circumstances (less than 10-fold of Fe^{2+}) [25], which will not influence the accurate assay of Fe^{2+}. Besides, it was observed that 2-fold excess of ascorbic acid (AA)

Table 1 Analytical figures of merit for Fe^{2+} detection

Linear range (μM)	R^2	Linear regression equation	RSD (%)	LOD (nM)	LOQ (nM)
0.080–2.5	0.9962	$\Delta F=0.25+6.12c_{\text{ferrous ion}}$	0.23[a]	24	80
5.0–100	0.9910	$\Delta F=9.5+1.04c_{\text{ferrous ion}}$	0.31[b]		

a and b: relative standard deviation of ΔF corresponding with 1.0 and 20 μM Fe^{2+}, respectively

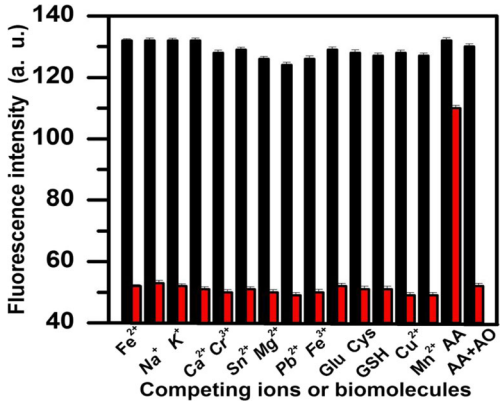

Fig. 4 Selectivity of the fluorescent sensor for Fe^{2+} over other representative competing ions or biomolecules in aqueous solution. Black column: fluorescence intensity of BSA-AuNCs with coexistence of 25 μM H_2O_2 in the absence of Fe^{2+}; red column: in the presence of Fe^{2+}. Concentration: Na^+, 400 mM; K^+, 240 mM; Ca^{2+}, Cr^{3+} and Mg^{2+}, 40 mM; Sn^{2+}, Pb^{2+}, 24 mM; Fe^{3+}, 4 mM; glucose, 16 mM; GSH, 8 mM; cysteine, 6.4 mM; Mn^{2+}, 480 μM; Cu^{2+}, 320 μM; ascorbic acid, 160 μM; The error bars represent the standard deviation of three measurements

would recover the fluorescence of the Fe^{2+} detection system, which was consistent with the results reported previously [26]. To eliminate the potential interference of AA in biological samples, a specific enzymatic reaction [27] was utilized in our experiments by the oxidation of AA to DHA with enzyme ascorbate oxidase (AO). The results demonstrate that AO effectively reduces the effect of AA for Fe^{2+} detection. Therefore, it is possible to use BSA-AuNCs as a fluorescent probe for Fe^{2+} detection in some biological samples.

Determination of Fe^{2+} in CSFs from Wistar rats model of Alzheimer's disease

Encouraged by the above-mentioned investigations, we evaluated if the fluorescent probe described here can be utilized to monitor Fe^{2+} in complex samples such as rat cerebrospinal fluids (CSFs), which is an ideal source that reflects the metabolic and pathological states of the central nervous system. It was reported that iron homeostasis in central nervous system is a very tightly regulated process [28], which is associated with aging-related progressive deterioration and with neurodegenerative disorders such as Alzheimer's disease. We obtained Wistar female rats model of AD and determined the Fe^{2+} content in CSFs (Sample 1–3), normal Wistar female rats CSFs were used as control (Sample 4–6). In addition, certain amount of standard solution of Fe^{2+} was added into the corresponding sample solutions for testing recovery. The results were shown in Table S1. It can be seen that a good recovery of 94.5–113 % was obtained, showing the good selectivity, high accuracy of the method. What's more, enhanced ferrous ion content in CSFs of AD model compared with control demonstrated the perturbed iron distribution and the important physiological role of iron in Alzheimer's disease.

Comparison with other methods

Comparative information from some studies on determination of Fe(II) by various methods for the figure of merits is given in Table 2. The suggested method has relatively low LOD and wide linear range for the Fe(II) compared to other methods reported in Table 2. What's more, our method does not need complex synthesis procedures and is more simple and cost-effective, which were favorable to the sensitive determination for Fe(II) in biological and other samples.

Conclusion

In summary, BSA-stabilized gold nanoclusters as a fluorescent probe for highly sensitive and selective determination of Fe^{2+} was presented. Under optimized conditions, we demonstrated the practical application of this assay by measuring the levels of Fe^{2+} in CSFs of Wistar female rats as AD model, indicating acceptable accuracy of the method. This strategy offers an alternative approach for low cost, simple, stable and sensitive detection of Fe^{2+}, and is beneficial for its applications including bioassays, nanotechnology, and clinical diagnostics.

Table 2 Figure of merits of comparable methods for determination of Fe(II)

Methods used	Analyticl ranges	LODs	Optimum pH value	Applicability to specific samples	References
fluorescent Probe: BDP-Cy-Tpy	0.1 to 7.0 μM	12 nM	7.4	HL-7702 cells	[29]
fluorescent probe : RhoNox-1	0.2 to 20 μM	0.2 μM	3.4–11.3	MCF-7 cells	[30]
colorimetric method	0 to 40 μM	2.94 μM	2–11	aqueous solutions of different metal ions	[31]
fluorescent probe: DansSQ	Not mentioned	3.6 μM	in ACN–H_2O (9:1, v/v)	not mentioned	[32]
fluorometric probe: BSA-AuNCs	0.08 to 100 μM	24 nM	pH 5.7	cerebrospinal fluids	Our work

Acknowledgments This work was supported by National Natural Science Foundation of China (21105057), Promotive Research Fund for Excellent Young and Middle-aged Scientist of Shandong Province (BS2013SW002) and Innovative Training Project for Undergraduate Students of Shandong Normal University.

References

1. Hentze MW, Muckenthaler MU, Galy B, Camaschella C (2010) Two to tango: regulation of mammalian iron metabolism. Cell 142:24
2. Brissot P, Ropert M, Lan CL, Loréal O (2012) Non-transferrin bound iron: a key role in iron overload and iron toxicity. Biochim Biophys Acta 1820:403
3. Vecchi C, Montosi G, Zhang KZ, Lamberti I, Duncan SA, Kaufman RJ, Pietrangelo A (2009) ER stress controls iron metabolism through induction of hepcidin. Science 325:877
4. Cao HY, Chen ZH, Zheng HZ, Huang YM (2014) Copper nanoclusters as a highly sensitive and selective fluorescence sensor for ferric ions in serum and living cells by imaging. Biosens Bioelectron 62:189
5. Chen YT, Jiang JZ (2013) *N*,*N*-di(2-pyridylmethyl)amino-modified porphyrinato zinc complexes. The "ON–OFF" fluorescence sensor for Fe^{3+}. Spectrochim Acta A Mol Biomol Spectrosc 116:418
6. Feldheim D (2000) Nanotechnology: flipping a molecular switch. Nature 408:45
7. Li G, Jin RC (2014) Gold nanocluster-catalyzed semihydrogenation: a unique activation pathway for terminal alkynes. J Am Chem Soc 136:11347
8. Lin CA, Yang TY, Lee CH, Huang SH, Sperling RA, Zanella M, Li JK, Shen JL, Wang HH, Yeh HI, Parak W, Chang WH (2009) Synthesis, characterization, and bioconjugation of fluorescent gold nanoclusters toward biological labeling applications. ACS Nano 3: 395
9. Hofmann CM, Essner JB, Baker GA, Baker SN (2014) Protein-templated gold nanoclusters sequestered within sol–gel thin films for the selective and ratiometric luminescence recognition of Hg^{2+}. Nanoscale 6:5425
10. Santhosh M, Chinnadayyala SR, Kakoti A, Goswami P (2014) Selective and sensitive detection of free bilirubin in blood serum using human serum albumin stabilized gold nanoclusters as fluorometric and colorimetric probe. Biosens Bioelectron 59:370
11. Chan PH, Chen YC (2012) Human serum albumin stabilized gold nanoclusters as selective luminescent probes for staphylococcus aureus and methicillin-resistant staphylococcus aureus. Anal Chem 84:8952
12. Lin H, Li LJ, Lei CY, Xu XH, Nie Z, Guo ML, Huang Y, Yao SZ (2013) Immune-independent and label-free fluorescent assay for Cystatin C detection based on protein-stabilized Au nanoclusters. Biosens Bioelectron 41:256
13. Park KS, Kim MI, Woo MA, Park HG (2013) A label-free method for detecting biological thiols based on blocking of Hg^{2+}-quenching of fluorescent gold nanoclusters. Biosens Bioelectron 45:65
14. Jin LH, Shang L, Guo SJ, Fang YX, Wen D, Wang L, Yin JY, Dong SJ (2011) Biomolecule-stabilized Au nanoclusters as a fluorescence probe for sensitive detection of glucose. Biosens Bioelectron 26: 1965
15. Cui ML, Liu JM, Wang XX, Lin LP, Jiao L, Zhang LH, Zheng ZY, Lin SQ (2012) Selective determination of cysteine using BSA-stabilized gold nanoclusters with red emission. Analyst 137:5346
16. Wang XX, Wu Q, Shan Z, Huang QM (2011) BSA-stabilized Au clusters as peroxidase mimetics for use in xanthine detection. Biosens Bioelectron 26:3614
17. Zhang N, Si YM, Sun ZZ, Li S, Li SY, Lin YH, Wang H (2014) Lab-on-a-drop: biocompatible fluorescent nanoprobes of gold nanoclusters for label-free evaluation of phosphorylation-induced inhibition of acetylcholinesterase activity towards the ultrasensitive detection of pesticide residues. Analyst 139:4620
18. Liu YL, Ai KL, Cheng XL, Huo LH, Lu LH (2010) Gold-nanocluster-based fluorescent sensors for highly sensitive and selective detection of cyanide in water. Adv Funct Mater 20:951
19. Xie JP, Zheng YG, Ying JY (2010) Highly selective and ultrasensitive detection of Hg^{2+} based on fluorescence quenching of Au nanoclusters by Hg^{2+}–Au^{+} interactions. Chem Commun 46:961
20. Chen TT, Hu YH, Cen Y, Chu X, Lu Y (2013) A dual-emission fluorescent nanocomplex of gold-cluster-decorated silica particles for live cell imaging of highly reactive oxygen species. J Am Chem Soc 135:11595
21. Tao Y, Wang Y, Rogers JT, Wang F (2014) Perturbed iron distribution in Alzheimer's disease serum, cerebrospinal fluid, and selected brain regions: a systematic review and meta-analysis. J Alzheimers Dis 42:679
22. Xie JP, Zheng YG, Ying JY (2009) Protein-directed synthesis of highly fluorescent gold nanoclusters. J Am Chem Soc 131:888
23. Liu DB, Chen WW, Tian Y, He S, Zheng WF, Sun JH, Wang Z, Jiang XY (2012) A highly sensitive gold-nanoparticle-based assay for acetylcholinesterase in cerebrospinal fluid of transgenic mice with Alzheimer's disease. Adv Healthcare Mater 1:90
24. Zheng J, Nicovich PR, Dickson RM (2007) Highly fluorescent noble metal quantum dots. Annu Rev Phys Chem 58:409
25. Melo TM, Larsen C, White LR, Aasly J, Sjobakk TE, Flaten TP, Sonnewald U, Syversen T (2003) Manganese, copper, and zinc in cerebrospinal fluid from patients with multiple sclerosis. Biol Trace Elem Res 93:1
26. Hu LZ, Deng L, Alsaiari S, Zhang DY, Khashab NM (2014) "Light-on" sensing of antioxidants using gold nanoclusters. Anal Chem 86:4989
27. Kim WS, Ye X, Rubakhin SS, Sweedler JV (2006) Measuring nitric oxide in single neurons by capillary electrophoresis with laser-induced fluorescence: use of ascorbate oxidase in diaminofluorescein measurements. Anal Chem 78:1859
28. Mesquita SD, Ferreira AC, Sousa JC, Santos NC, Correia-Neves M, Sousa N, Palha JA, Marques F (2012) Modulation of iron metabolism in aging and in Alzheimer's disease: relevance of the choroid plexus. Front Cell Neurosci 6:1
29. Li P, Fang LB, Zhou H, Zhang W, Wang X, Li N, Zhong HB, Tang B (2011) A New ratiometric fluorescent probe for detection of Fe^{2+} with high sensitivity and its intracellular imaging applications. Chem Eur J 17:10520
30. Hirayama T, Okuda K, Nagasawa H (2013) A highly selective turn-on fluorescent probe for iron(II) to visualize labile iron in living cells. Chem Sci 4:1250
31. Kim H, Na YJ, Song EJ, Kyung KKB, Bae JM, Kim C (2014) A single colorimetric sensor for multiple target ions: the simultaneous detection of Fe^{2+} and Cu^{2+} in aqueous media. RSC Adv 4:22463
32. Praveen L, Reddy MLP, Varma RL (2010) Dans SQ can be used as turn-on fluorescent sensor for Fe^{2+}. Tetrahedron Lett 51:6626